

Multiple scattering effects in Glauber model descriptions of single-nucleon removal reactions

Rui-Ying Chen,¹ Dan-Yang Pang,^{1,2,*} Cen-Xi Yuan,³ Yi-Ping Xu,⁴
Wen-Di Chen,¹ Wen-Long Hai,¹ Jing-Jing Yan,¹ and Wei-Jia Kong¹

¹*School of Physics, Beihang University, Beijing 100191, China*

²*Beijing Key Laboratory of Advanced Nuclear Materials and Physics, Beihang University, Beijing 100191, China*

³*Sino-French Institute of Nuclear Engineering and Technology, Sun Yat-Sen University, Zhuhai 519082, China*

⁴*School of Nuclear Science and Engineering, North China Electric Power University, Beijing 102206, China*

The Glauber/eikonal model is a widely used tool for study of intermediate- and high-energy nuclear reactions. When calculating the Glauber/eikonal model phase-shift functions, the optical limit approximation (OLA) is often used. The OLA neglects the multiple scattering processes of the constituent nucleons in the projectile and the targets nuclei. It is remedied by the nucleon-target version of the Glauber model (NTG) proposed by B. Abu-Ibrahim and Y. Suzuki. The NTG method has been found to improve the description of the elastic scattering angular distributions and the total reaction cross sections of some light heavy-ion systems with respect to the OLA. In this work, we study the single-nucleon removal reactions (SNRR) induced by Carbon isotopes on ^{12}C and ^9Be targets using both the NTG method and the OLA. Reduction factors (RFs) of the single proton/neutron spectroscopic factors are obtained by comparing the experimental and theoretical SNRR cross sections. It is found that, on average, the RFs obtained with the NTG method is smaller than those using the OLA by 7.8%. The differences are larger when the incident energies are lower and/or the separation energies of the removed nucleons are larger. But the RFs values still have a strong dependence on the neutron-proton asymmetry ΔS of the projectile nuclei.

Keywords: Glauber model of nuclear reactions, single-nucleon removal reactions, spectroscopic factors

I. INTRODUCTION

Measurements and theoretical analysis of single-nucleon removal reactions are of great value for studies of single-particle strengths of atomic nuclei, which are quantitatively represented by spectroscopic factors (SFs) [1]. It is well-known that the SFs extracted from $(e, e'p)$ and single-nucleon transfer reactions are found to be 30% – 50% smaller than those predicted by configuration interaction shell model (CISM) [2, 3]. Such reduction or quenching of SFs, represented by the quenching factors, R_s , is supposed to be originated from the limited model spaces and insufficient treatment of the nucleon-nucleon correlations in the traditional CISM [4, 5]. Unlike the results from $(e, e'p)$ reactions, from single-nucleon transfer reactions, and from $(p, 2p)$ and (p, pn) reactions [2, 3, 6, 7], where the R_s values of different nuclei are nearly constant, the quenching factors from intermediate energy single-nucleon removal reactions are found to depend almost linearly with the proton-neutron asymmetry of the atomic nuclei, ΔS ($\Delta S = S_p - S_n$ for proton removal and $\Delta S = S_n - S_p$ for neutron removal with S_n and S_p being the neutron and proton separation energies in the ground states of the projectile nuclei, respectively) [8, 9]. For cases when ΔS is larger than around 20 MeV, which correspond to removal of strongly bound nucleons, the R_s values decrease to about 0.3; however, when ΔS is smaller than around -20 MeV, which corresponds to removal of weakly-bound nucleons, the R_s values are close to unity. The reasons why such a clear linear dependence is seen in results of intermediate-energy single-nucleon removal reactions are still not known. Since most of the single-nucleon removal reactions are ana-

lyzed with the Glauber model, validity of the eikonal/Glauber model [8–10] has been put under question [11].

Because of its simplicity, the optical limit approximation (OLA) is often used in the eikonal/Glauber model analysis of the intermediate- or high-energy nuclear reactions [10, 12, 13]. With the OLA, only the first-order term of the expansion of the full Glauber phase shift is taken into account. Higher-order interactions, such as multiple scattering processes of nucleon-nucleon scattering are neglected [14]. In Ref. [15], B. Abu-Ibrahim and Y. Suzuki found that although the Glauber model with the OLA can reasonably reproduce the total reaction cross sections of some stable ions on ^9Be , ^{12}C , ^{27}Al targets, it failed to reproduce the reaction cross sections and elastic scattering angular distributions of unstable nuclei. For this, they proposed to calculate the projectile-target phase shifts using nucleon-target interactions in Glauber model calculations. This so called NTG model (nucleon-target version of the Glauber model) has been found to improve the description of the reaction cross sections and the elastic scattering angular distributions data considerably [15–17]. However, to our knowledge, effects of the NTG method on the reduction factors of single particle strengths from analysis of single-nucleon knockout reactions has not been studied yet. In this work, we study how much the R_s values of single-nucleon knockout reactions will change when the NTG method is used instead of the OLA. Since the NTG method includes multiple scattering effects in the phase-shift functions of the colliding systems with respect to the OLA, we expect this work may give us information about how much the multiple scattering effects will affect the description of single nucleon removal reactions using the Glauber model.

This paper is organized as the following: the NTG method and the OLA of the Glauber model are briefly introduced in section II; results of our calculations are given in section III,

* Corresponding author: dypang@buaa.edu.cn

which include 1) examination of the NTG method about its reproduction of the elastic scattering and total reaction cross section data. The cases studied are the angular distributions of ^{12}C elastic scattering from a carbon target at incident energies from 30 to 200 MeV/u and the $^{12}\text{C}+^{12}\text{C}$ total reaction cross sections from 20 to 1000 MeV/nucleon, 2) detailed study of the NTG method on single-nucleon removal at different incident energies, the case studied here is the $(^{19}\text{C}, ^{18}\text{C})$ reaction, and 3) effects of the NTG method on the reduction factors of the single particle strengths. The cases studied are single nucleon removal cross sections of carbon isotopes $^{9,10,12-20}\text{C}$ on ^9Be and carbon targets within 43-250 MeV/nucleon incident energies. The range of ΔS covered in these reactions is from -26.6 to 19.9 MeV. All results are compared with those of the OLA calculations in order to explicit the influence of multiple scattering effects in these reactions; the conclusions are given in section IV.

II. THE NTG METHOD AND THE OLA

The NTG method was introduced in Refs. [15, 16]. That the NTG method includes some multiple scattering effects other than the OLA has been implicated in Ref. [14] but not explicated. This will be made in this section. Most of the formula can be found in Ref. [14]. For the convenience of the readers, we recapitulate the necessary ones here. Let us start from the phase-shift function of a nucleon-target system, χ_{NT} , which is defined in the Glauber model framework as [14]:

$$e^{i\chi_{NT}(\mathbf{b})} = \langle \Phi_0^T | \prod_{j=1}^{A_T} [1 - \Gamma_{NN}(\mathbf{b} - \mathbf{s}_j)] | \Phi_0^T \rangle, \quad (1)$$

where \mathbf{b} is the impact factor vector, \mathbf{s}_j is the projection vector of the position of the j th nucleon in the target nucleus on the x - y plane (the beam direction being the z -axis), Γ_{NN} is the nucleon-nucleon (NN) profile function, which is the Fourier transform of the NN scattering amplitude, and $|\Phi_0\rangle$ is the wave function of the target nucleus, which has a mass number A_T . When an independent particle model wave function is used, which is usually assumed in Glauber model calculations, the density of the target nucleus can be written as [14]:

$$|\Phi_0^T(\mathbf{r}_1, \mathbf{r}_2, \dots, \mathbf{r}_{A_T})|^2 = \prod_{j=1}^{A_T} n_j(\mathbf{r}_j), \quad (2)$$

where $n_j(\mathbf{r}_j)$ stands for the normalized density distribution of the j th nucleon in the target nucleus. The nucleon density distribution is then

$$\rho_T(\mathbf{r}) = \sum_{j=1}^{A_T} n_j(\mathbf{r}). \quad (3)$$

With an uncorrelated wave function satisfying Eq. 2, the nucleon-target phase shift function has the form [14]:

$$e^{i\chi_{NT}(\mathbf{b})} = \prod_{j=1}^{A_T} \left[1 - \int d\mathbf{r} n_j(\mathbf{r}) \Gamma_{NN}(\mathbf{b} - \mathbf{s}) \right], \quad (4)$$

where \mathbf{s} is the projection of \mathbf{r} on the x - y plane. When the range of the NN interaction is smaller than the radius of the target nucleus, which is satisfied in most cases, the integral $\int d\mathbf{r} n_j(\mathbf{r}) \Gamma_{NN}(\mathbf{b} - \mathbf{s})$ will be smaller than unity. Then the following approximation could be made [14]:

$$1 - \int d\mathbf{r} n_j(\mathbf{r}) \Gamma_{NN}(\mathbf{b} - \mathbf{s}) \approx e^{-\int d\mathbf{r} n_j(\mathbf{r}) \Gamma_{NN}(\mathbf{b} - \mathbf{s})}. \quad (5)$$

One then get the nucleon-target phase shift of the OLA [14]:

$$\begin{aligned} e^{i\chi_{NT}^{\text{OLA}}(\mathbf{b})} &= \prod_{j=1}^{A_T} \exp \left[- \int d\mathbf{r} n_j(\mathbf{r}) \Gamma_{NN}(\mathbf{b} - \mathbf{s}) \right] \\ &= \exp \left[- \sum_{j=1}^{A_T} \int d\mathbf{r} n_j(\mathbf{r}) \Gamma_{NN}(\mathbf{b} - \mathbf{s}) \right] \\ &= \exp \left[- \int d\mathbf{r} \rho_T(\mathbf{r}) \Gamma_{NN}(\mathbf{b} - \mathbf{s}) \right]. \end{aligned} \quad (6)$$

This results in the nucleon-nucleus phase-shift function using the OLA being:

$$\chi_{NT}^{\text{OLA}}(\mathbf{b}) = i \int d\mathbf{r} \rho_T(\mathbf{r}) \Gamma_{NN}(\mathbf{b} - \mathbf{s}). \quad (7)$$

Note that in Eqs. (1) and (4), multiple scattering terms appear through cumulant expansions of the phase-shift functions. However, after applying the approximation of Eq. (5) in Eq. (4), the resulting nucleon-nucleus phase-shift in Eq. (7) contains no multiple scattering terms anymore.

Similar to the nucleon-nucleus case in Eq. (1), the nucleus-nucleus phase shift function, $\chi_{PT}(\mathbf{b})$, for a composite projectile and a target nucleus is:

$$e^{i\chi_{PT}(\mathbf{b})} = \langle \Phi_0^P \Phi_0^T | \prod_{i=1}^{A_P} \prod_{j=1}^{A_T} [1 - \Gamma_{NN}(\mathbf{b} + \mathbf{s}_i^P - \mathbf{t}_j^T)] | \Phi_0^P \Phi_0^T \rangle, \quad (8)$$

where Φ_0^P is the many-body wave functions of the projectile (with a mass number A_P) in its ground state. The integrals are over the coordinates of all the nucleons i and j in the projectile and target nuclei, whose coordinates are \mathbf{r}_i and \mathbf{r}_j , respectively. \mathbf{s}_i^P , and \mathbf{t}_j^T are their projections on the x - y plane. The nucleus-nucleus phase shift in this equation contains contributions from single collisions and all order multiple scattering among the constituent nucleons in the projectile and target nuclei. Equation (8) is cumbersome to evaluate microscopically even if it is possible. So the optical limit approximation is usually used and the phase shift function with this approximation is [14]:

$$\chi_{PT}^{\text{OLA}}(\mathbf{b}) = i \int d\mathbf{r}_P \rho_P(\mathbf{r}_P) \int d\mathbf{r}_T \rho_T(\mathbf{r}_T) \Gamma_{NN}(\mathbf{b} + \mathbf{s}^P - \mathbf{t}^T), \quad (9)$$

where ρ_P and ρ_T are the nucleon density distributions of the projectile and nuclei, respectively, \mathbf{r}_P and \mathbf{r}_T are the positions of their constituent nucleons, whose projections on the

148 x - y plane are \mathbf{s}^P and \mathbf{t}^T respectively. As in the nucleon-
 149 nucleus case in Eq. (7), only one-step NN collisions con-
 150 tribute to this phase shift. Contributions from multiple scat-
 151 terings are missing, which could be, at least partially, recov-
 152 ered by the nucleon-target version of the Glauber model (the
 153 NTG method) proposed by Abu-Ibrahim and Suzuki [14–17].

154 The idea of the NTG method is to replace $\prod_{j \in T} [1 -$
 155 $\Gamma_{NN}(\mathbf{b} + \mathbf{s}_i^P - \mathbf{t}_j^T)] |\Phi_0^T\rangle$ for each nucleon i in the projec-
 156 tile in Eq. (8) by

$$\begin{aligned} & |\Phi_0^T\rangle \langle \Phi_0^T| \prod_{j=1}^{A_T} [1 - \Gamma_{NN}(\mathbf{b} + \mathbf{s}_i^P - \mathbf{t}_j^T)] |\Phi_0^T\rangle \\ &= [1 - \Gamma_{NT}(\mathbf{b} + \mathbf{s}_i^P)] |\Phi_0^T\rangle, \end{aligned} \quad (10)$$

159 where $\Gamma_{NT}(\mathbf{b} + \mathbf{s}_i^P)$ is the profile function of its collision
 160 with the target nucleus. The nucleus-nucleus phase shift with
 161 the NTG method then takes the form [14]:

$$e^{i\chi_{PT}^{\text{NTG}}(\mathbf{b})} = \langle \Phi_0^P | \prod_{i=1}^{A_P} [1 - \Gamma_{NT}(\mathbf{b} + \mathbf{s}_i^P)] | \Phi_0^P \rangle. \quad (11)$$

163 Following the same procedure of obtaining the Eq. (7),
 164 the phase shift of the projectile-target system with the NTG
 165 method is:

$$\chi_{PT}^{\text{NTG}}(\mathbf{b}) = i \int d\mathbf{r} \rho_P(\mathbf{r}) \Gamma_{NT}(\mathbf{b} + \mathbf{s}). \quad (12)$$

167 The nucleon-target profile function, Γ_{NT} , defined in Eq.
 168 (10) has contributions from multiple scattering of the nucleon
 169 in the projectile from all the constituent nucleons in the tar-
 170 get nucleus, which can be seen from the following cumulant
 171 expansion:

$$\begin{aligned} & \Gamma_{NT}(\mathbf{b} + \mathbf{s}_i^P) \\ & \equiv 1 - \langle \Phi_0^T | \prod_{j=1}^{A_T} [1 - \Gamma_{NN}(\mathbf{b} + \mathbf{s}_i^P - \mathbf{t}_j^T)] | \Phi_0^T \rangle \\ &= \sum_{j=1}^{A_T} \langle \Phi_0^T | \Gamma_{ij} | \Phi_0^T \rangle - \sum_{j=1}^{A_T} \sum_{k=1}^{A_T} \langle \Phi_0^T | \Gamma_{ij} \Gamma_{ik} | \Phi_0^T \rangle \\ &+ \sum_{j=1}^{A_T} \sum_{k=1}^{A_T} \sum_{l=1}^{A_T} \langle \Phi_0^T | \Gamma_{ij} \Gamma_{ik} \Gamma_{il} | \Phi_0^T \rangle - \dots (j \neq k \neq l) \end{aligned} \quad (13)$$

176 Here $\Gamma_{im} \equiv \Gamma_{NN}(\mathbf{b} + \mathbf{s}_i^P - \mathbf{t}_m^T)$ is the profile function of the
 177 collision between the i th nucleon in the projectile and the m th
 178 nucleon in the target nucleus ($m = j, k, l, \dots$). The first term
 179 in this expansion represents single collisions with the target
 180 nucleons, while the other terms represent multiple scattering,
 181 namely, succession of collisions between the incident nucleon
 182 and target nucleons [18]. Assuming again that the target wave
 183 function Φ_0^T is uncorrelated as in Eq. (2), the above expansion

184 can also be written as:

$$\begin{aligned} & \Gamma_{NT}(\mathbf{b} + \mathbf{s}_i^P) \\ &= \sum_{j=1}^{A_T} \langle \Phi_0^T | \Gamma_{ij} | \Phi_0^T \rangle - \frac{1}{2!} \left[\sum_{j=1}^{A_T} \langle \Phi_0^T | \Gamma_{ij} | \Phi_0^T \rangle \right]^2 \\ &+ \frac{1}{3!} \left[\sum_{j=1}^{A_T} \langle \Phi_0^T | \Gamma_{ij} | \Phi_0^T \rangle \right]^3 - \dots \end{aligned} \quad (14)$$

188 Using again the optical limit approximation to the term
 189 $\sum_{j \in T} \langle \Phi_0^T | \Gamma_{ij} | \Phi_0^T \rangle$ [14], we get:

$$\sum_{j=1}^{A_T} \langle \Phi_0^T | \Gamma_{ij} | \Phi_0^T \rangle = \int d\mathbf{r}_T \rho_T(\mathbf{r}_T) \Gamma_{NN}(\mathbf{b} + \mathbf{s}_i^P - \mathbf{t}^T). \quad (15)$$

191 where \mathbf{t}^T is the projection of the vector \mathbf{r}_T on the x - y plane.
 192 The nucleon-target profile function is then:

$$\begin{aligned} & \Gamma_{NT}(\mathbf{b} + \mathbf{s}_i^P) \\ &= \int d\mathbf{r}_T \rho_T(\mathbf{r}_T) \Gamma_{NN}(\mathbf{b} + \mathbf{s}_i^P - \mathbf{t}) - \\ & \frac{1}{2!} \left[\int d\mathbf{r}_T \rho_T(\mathbf{r}_T) \Gamma_{NN}(\mathbf{b} + \mathbf{s}_i^P - \mathbf{t}) \right]^2 + \dots \\ &= 1 - \exp \left[- \int d\mathbf{r}_T \rho_T(\mathbf{r}_T) \Gamma_{NN}(\mathbf{b} + \mathbf{s}_i^P - \mathbf{t}) \right], \end{aligned} \quad (16)$$

198 Substituting this Γ_{NT} in Eq. (12), we get the nucleus-nucleus
 199 phase shift function of the NTG model:

$$\begin{aligned} & \chi_{PT}^{\text{NTG}}(\mathbf{b}) = i \int d\mathbf{r}_P \rho_P(\mathbf{r}_P) \\ & \times \left\{ 1 - \exp \left[- \int d\mathbf{r}_T \rho_T(\mathbf{r}_T) \Gamma_{NN}(\mathbf{b} + \mathbf{s} - \mathbf{t}) \right] \right\}. \end{aligned} \quad (17)$$

203 Notes that if only the first term of Eq. (16) is used in Eq. (12),
 204 the NTG phase shift will reduce to the one with the OLA in
 205 Eq. (9). Since the higher order terms in Eq. (16) represent the
 206 multiple scattering of the projectiles from the nucleons in the
 207 target nucleus, inclusion of these terms in Eq. (17) suggests
 208 that the phase shift of the NTG method recover some multi-
 209 ple scattering effects that are missing with the OLA. A sym-
 210 metrized version of the NTG phase shift is often used [15]:

$$\begin{aligned} & \chi_{PT}^{\text{NTG}}(\mathbf{b}) = \frac{i}{2} \int d\mathbf{r}_P \rho_P(\mathbf{r}_P) \left\{ 1 - \right. \\ & \exp \left[- \int d\mathbf{r}_T \rho_T(\mathbf{r}_T) \Gamma_{NN}(\mathbf{b} + \mathbf{s} - \mathbf{t}) \right] \left. \right\} \\ & + \frac{i}{2} \int d\mathbf{r}_T \rho_T(\mathbf{r}_T) \left\{ 1 - \right. \\ & \exp \left[- \int d\mathbf{r}_P \rho_P(\mathbf{r}_P) \Gamma_{NN}(\mathbf{b} + \mathbf{t} - \mathbf{s}) \right] \left. \right\}. \end{aligned} \quad (18)$$

However, the phase-shifts calculated with Eqs. (17) and (18) are often very close to each other [15, 16].

The profile function Γ_{NN} in the both the OLA and the NTG method calculations is parameterized in a Gaussian form:

$$\Gamma_{pN}(\mathbf{b}) = \frac{1 - i\alpha_{pN}}{4\pi\beta_{pN}} \sigma_{pN}^{\text{tot}} \exp\left(-\frac{\mathbf{b}^2}{2\beta_{pN}}\right), \quad (19)$$

where the Γ_{NN} parameters σ_{pN}^{tot} , α_{pN} , and β_{pN} are the proton-nucleon total cross section, the ratio of the real to imaginary part of the p - N scattering amplitudes, and the corresponding slope parameter [19], respectively. Due to the lack of experimental data on neutron-neutron scattering, Γ_{pp} is commonly used instead of Γ_{NN} . In this work, σ_{pN}^{tot} are taken from Ref. [20], which is parameterized by fitting the experimental data from Ref. [21], the α_{pN} parameters are taken from those tabulated from Ref. [19] for a range of incident energies from 100 to 2200 MeV/u. If the beam energy is lower than 100 MeV/u, we take the value corresponding to lowest energy from the table. The finite range slope parameters β_{pN} are taken to be 0.125 fm², in accordance with systematic studies of single-nucleon removal reaction [10, 12, 22].

III. COMPARISONS BETWEEN THE NTG METHOD AND OLA IN GLAUBER MODEL CALCULATIONS

The main purpose of this paper is to study how the single-particle strengths from single-nucleon removal cross sections change when the NTG method, instead of the OLA, is used in the Glauber model calculations. In Ref. [23], T. Nagashisa and W. Horiuchi demonstrated the effectiveness of the NTG by comparing the description of the total reaction cross sections using the full Glauber model calculation, the NTG method, and the OLA for cases of $^{12,20,22}\text{C}$ on a ^{12}C target at various incident energies. In this work, our main purpose is to study how much the single-nucleon removal cross sections (σ_{-1N}) will change when the NTG method instead of the OLA is used. Before calculating σ_{-1N} , we need to firstly compare our calculations for the elastic scattering angular distributions and total reaction cross sections with experimental data and with predictions with the OLA. The calculations are made for the $^{12}\text{C}+^{12}\text{C}$ system. By doing so, we also verify the effectiveness of the Γ_{NN} parameters used in our calculations, which are further used in the calculations of σ_{-1N} . The single-nucleon removal reactions are calculated using a modified version of the computer code MOMDIS [24].

A. Elastic scattering angular distributions and total reaction cross sections

The angular distributions of ^{12}C elastic scattering from a ^{12}C target at 30, 85, 120, and 200 MeV/nucleon are calculated with both the OLA and the NTG method. The results are shown in Fig. 1 together with the experimental data. Clearly, the NTG improved the description of the $^{12}\text{C}+^{12}\text{C}$ elastic scattering considerably with respect to the OLA, especially

when the incident energy is below around 100 MeV/nucleon. This can be expected because the multiple scattering effect, which are included in the NTG method but not in the OLA, should be more important at low incident energies than at higher incident energies. Note that other corrections due to, for instance, the antisymmetrization of the projectile and target wavefunctions [25], the Fermi motion of the nucleons in the colliding nuclei [26], distortion of the trajectories [27], can also affect the low-energy cross sections. More complete calculations taking these aspect together might be an interesting subject for future.

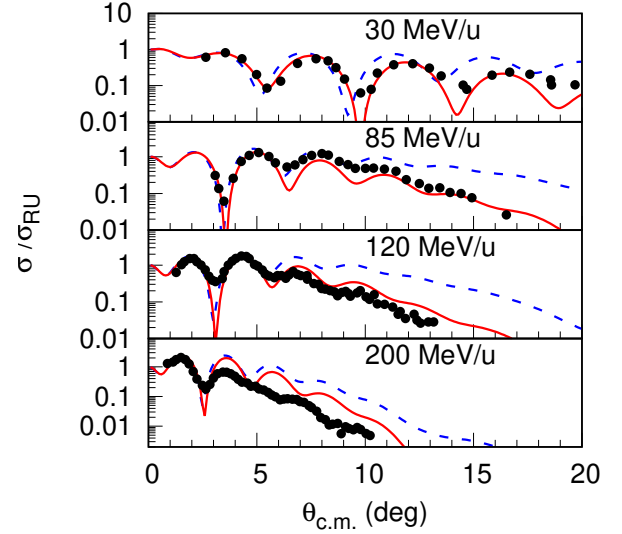


Fig. 1. Elastic scattering angular distributions of ^{12}C on a carbon target at incident energies of 30, 85, 120, and 200 MeV/nucleon. The red solid and blue dashed curves are results of Glauber model calculations with the NTG method and the OLA, respectively. The dots are experimental data from Refs. [28, 29].

Comparison between the NTG and OLA predictions to the total reaction cross sections of the $^{12}\text{C}+^{12}\text{C}$ system is shown in Fig. 2. Again, we see that results of the NTG method have better agreement with the experiment data than those of the OLA, especially for the incident energies at several tens of MeV/nucleon and above, where most of the one-nucleon removal cross section data were measured [9]. In both elastic scattering and total reaction cross section calculations, the proton and neutron density distributions of the ^{12}C nucleus are taken to be a Gaussian form with a root-mean-square radius of 2.32 fm [9], which is very close to the 2.33 ± 0.01 fm from elastic electron scattering data [30].

Note that the Γ_{NN} parameters are the same in both NTG and OLA calculations. The only difference between these two methods is that the former method introduced the multiple scattering effects in the calculation of eikonal phase functions. The improvement provided by the NTG method in the description of elastic scattering angular distributions and the total reaction cross sections suggests that nuclear medium effects, such as the multiple scattering effect studied here, should be taken into account in Glauber model description of the nuclear reactions induced by heavy-ions. In the fol-

lowing section, we study how the NTG method could affect the theoretical predictions of the single-neutron removal cross sections and the single particle strengths obtained from the experimental data.

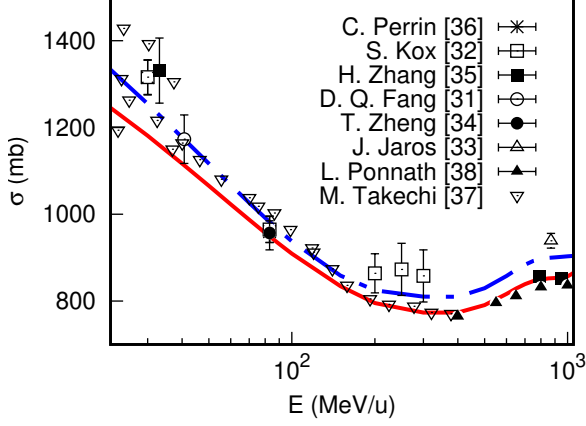


Fig. 2. Reaction cross sections of ^{12}C on a carbon target. The red solid and blue dash-dotted curves are results of Glauber model calculations with the NTG method and the OLA, respectively. The symbols represent experimental data from Ref. [31–38].

B. Single-nucleon removal cross sections at different incident energies

In an inclusive single-nucleon removal reaction, $A(a, b)X$, where only the core nucleus b ($A_b = A_a - 1$) is detected, two processes may happen: the diffraction dissociation and stripping, which correspond to the valence neutron escaped or being captured by the target nucleus, respectively. Within the Glauber model framework, their cross sections, σ_{sp}^{dd} and σ_{sp}^{str} , respectively, are calculated by: [39]:

$$\sigma_{sp}^{dd} = \frac{1}{2j+1} \sum_m \int d\mathbf{b} [\langle \psi_{nljm} | |1 - S_v S_c|^2 | \psi_{nljm} \rangle - \sum_{m'} |\langle \psi_{nljm'} | (1 - S_v S_c) | \psi_{nljm} \rangle|^2], \quad (20)$$

and

$$\sigma_{sp}^{str} = \frac{1}{2j+1} \sum_m \int d\mathbf{b} |S_c|^2 \times \langle \psi_{nljm} | (1 - |S_v|^2) | \psi_{nljm} \rangle. \quad (21)$$

Here $S_c = e^{i\chi_{cT}}$ and $S_v = e^{i\chi_{vT}}$ are the core-target and the valence nucleon-target S -matrix, respectively. The valence nucleon-target phase shift function χ_{vT} is calculated with Eq. (7), and the core-target phase shift function χ_{cT} is calculated according to Eq. (9) for the OLA and Eq. (18) for the NTG method; \mathbf{b} is the impact factor vector of the projectile in the plane perpendicular to the beam direction, ψ_{nljm} is the single-particle wave function (SPWF) with n , l , and j be-

ing the principal, the angular momentum, and the total angular momentum numbers respectively, and m is the projection of j . Equations (7, 9, 17 and 18) are about nuclear phase-shift only. For charged particles, one also has to include the Coulomb phase-shift [24]:

$$\chi_C = 2\eta \ln(kb), \quad (22)$$

where $\eta = Z_1 Z_2 e^2 \mu / \hbar^2 k$ is the Sommerfeld parameter with Z_1 and Z_2 being the charge numbers of the two colliding particles, whose reduced mass is μ , and k being the wave number in the center of mass system. The single-particle wave functions are associated with the specific states of the core with spin I_b and the composite nuclei with spin I_a by spectroscopic factors, $(C^2S)_{I_a I_b, nlj}$. So, the single-particle cross section of removal of a nucleon from the ground state of a projectile leaving the core nucleus in a specific state with the SPWF having quantum numbers nlj is:

$$\sigma_{sp}(I_a I_b, nlj) = \left(\frac{A}{A-1} \right)^N (C^2S)_{I_a I_b, nlj} \times (\sigma_{sp}^{dd} + \sigma_{sp}^{str}),$$

where the $(A/A-1)^N$ factor is for the center-of-mass corrections to the spectroscopic factor C^2S , and $N = 2n + l$ is the number of oscillator quanta associated with the major shell of the removed particle (the minimum value of n is taken to be zero).

Experimentally, single-nucleon removal cross sections are usually measured inclusively, namely, only the core nucleus b is measured without discriminating its energy states. Correspondingly, theoretical calculations for these measurements should also include the contributions from all the bound excited states of the core nucleus b [10], which correspond to summation of all the single-particle cross sections associated with all possible single particle wave functions:

$$\sigma_{-1N}^{\text{th}} = \sum_{nlj, I_b} \sigma_{sp}(I_a I_b, nlj). \quad (23)$$

In order to see how much difference the NTG method predicts the single-nucleon removal cross sections with respect to the OLA, we study the (^{19}C , ^{18}C) reaction on a carbon target at 50, 100, 200, and 400 MeV/nucleon incident energies. The excited states of the ^{18}C nucleus, the associated single particle wave functions, and their corresponding shell model predicted spectroscopic factors are taken to be the same as those in Ref. [12]. The single particle wave functions are calculated with single particle potentials of Woods-Saxon forms with the depths adjusted to provide the experimental separation energies of the valence nucleon, and the radius and diffuseness parameters are taken to be $r_0 = 1.03$ fm and $a = 0.65$ fm consistent with Ref. [40], respectively. The results are shown in Table. 1. The ratios of the inclusive one-neutron removal cross sections calculated with the NTG method and the OLA are depicted in Fig. 3.

It is interesting to observe that:

1. the one-nucleon removal cross sections calculated with the NTG method is larger than those with the OLA within the whole energy range from 50 to 400 MeV/nucleon,

TABLE 1. Single neutron removal cross sections of ^{19}C on a carbon target at incident energies of 50, 100, 200, and 400 MeV/nucleon calculated with the NTG method, $\sigma_{-1n}^{\text{NTG}}$, and the OLA, $\sigma_{-1n}^{\text{OLA}}$. The state of the core nucleus and their corresponding single-nucleon spectroscopic factors are taken from Ref. [12].

E_{inc}	E_x	J^π	nlj	C^2S	$\sigma_{-1n}^{\text{OLA}}$	$\sigma_{-1n}^{\text{NTG}}$	$\sigma_{-1n}^{\text{NTG}}/\sigma_{-1n}^{\text{OLA}}$
50	0.000	0^+	$1s_{1/2}$	0.580	108.51	117.76	1.085
	2.144	2^+	$0d_{5/2}$	0.470	13.69	16.60	1.213
	3.639	2^+	$0d_{5/2}$	0.104	2.49	3.06	1.230
	3.988	0^+	$1s_{1/2}$	0.319	15.05	17.89	1.189
	4.915	3^+	$0d_{5/2}$	1.523	32.00	39.69	1.240
	4.975	2^+	$0d_{5/2}$	0.922	19.27	23.89	1.240
	Inclusive				191.01	218.90	1.146
100	0.000	0^+	$1s_{1/2}$	0.580	90.80	94.76	1.044
	2.144	2^+	$0d_{5/2}$	0.470	13.47	14.83	1.101
	3.639	2^+	$0d_{5/2}$	0.104	2.51	2.78	1.106
	3.988	0^+	$1s_{1/2}$	0.319	14.22	15.53	1.091
	4.915	3^+	$0d_{5/2}$	1.523	32.80	36.38	1.109
	4.975	2^+	$0d_{5/2}$	0.922	19.77	21.91	1.108
	Inclusive				173.58	186.18	1.073
200	0.000	0^+	$1s_{1/2}$	0.580	66.90	69.71	1.042
	2.144	2^+	$0d_{5/2}$	0.470	12.07	13.25	1.098
	3.639	2^+	$0d_{5/2}$	0.104	2.31	2.55	1.103
	3.988	0^+	$1s_{1/2}$	0.319	12.11	13.15	1.086
	4.915	3^+	$0d_{5/2}$	1.523	30.70	33.99	1.107
	4.975	2^+	$0d_{5/2}$	0.922	18.50	20.49	1.108
	Inclusive				142.59	153.14	1.074
400	0.000	0^+	$1s_{1/2}$	0.580	58.28	61.34	1.053
	2.144	2^+	$0d_{5/2}$	0.470	11.26	12.71	1.128
	3.639	2^+	$0d_{5/2}$	0.104	2.17	2.47	1.138
	3.988	0^+	$1s_{1/2}$	0.319	11.12	12.33	1.109
	4.915	3^+	$0d_{5/2}$	1.523	29.03	33.17	1.143
	4.975	2^+	$0d_{5/2}$	0.922	17.51	20.01	1.143
	Inclusive				129.37	142.03	1.098

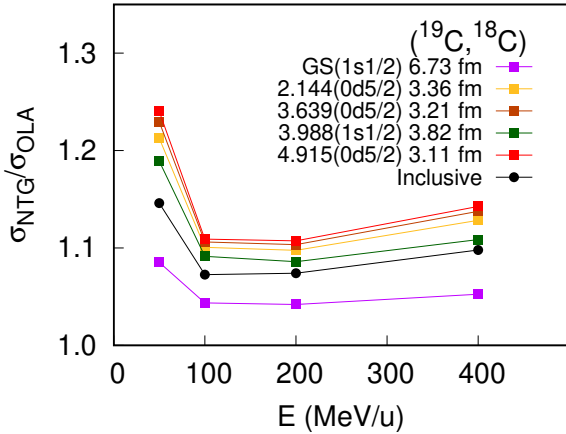


Fig. 3. Ratios of the NTG and OLA predicted single particle and the inclusive cross sections of the $(^{19}\text{C}, ^{18}\text{C})$ reactions at incident energies of 50, 100, 200, and 400 MeV/nucleon. Indicated in the figure are the excitation energies of the core nucleus ^{18}C , the nlj values, and the rms radii of the corresponding single-nucleon wave functions.

2. Such differences are larger at incident energies smaller than around 100 MeV/nucleon, almost constant around 100-200 MeV/nucleon, and increase slightly when the incident energy is larger than around 200 MeV/nucleon,

3. As is shown in Fig. 3, the differences are also bigger when the root-mean-square radius of the single particle wave function is smaller, which means that the NTG method is especially important for one-neutron removal cross sections of a given reaction when the single nucleon is tightly bound.

From these results, one may estimate that the NTG effect on the one-neutron removal cross sections is most important when the incident energy is low and the removed nucleon is tightly bound. In the following subsection, we study how the spectroscopic factors extracted from the experimental data and their reduction factors change when the NTG method instead of the OLA is used.

C. Reduction factors of single particle strengths

The spectroscopic factors in Eq. (23) are often taken from configuration interaction shell model (CISM) calculations in calculating the one-nucleon removal cross sections. Due to limited model spaces and insufficient treatment of nucleon-nucleon correlations, It is well-known that the CISM predicted SFs are usually larger than the experimental ones. Reduction factors of the SFs, R_s , which are ratios between the experimental and theoretical SFs, are defined to quantify such differences. For the case of inclusive single-nucleon knockout reactions, the reduction factors are defined as the ratios between the experimental and theoretical cross sections [8, 9]:

$$R_s = \sigma_{-1N}^{\text{exp}} / \sigma_{-1N}^{\text{th}}.$$

For nuclei that have more than one sets of experimental data available, a weighted mean of the R_s values for each measurement is used [41]:

$$\overline{R_s} = \frac{\sum_i (R_s)_i w_i}{\sum_i w_i}, \quad (24)$$

where the weights are defined by the errors of the individual R_s values $(\Delta R_s)_i$:

$$w_i = \left[\frac{1}{(\Delta R_s)_i} \right]^2,$$

and the errors of the averaged $\overline{R_s}$ is:

$$\Delta \overline{R_s} = \frac{1}{\sqrt{\sum_i w_i}}.$$

Using the method described in the previous subsection, we analysis a series of single-nucleon removal reaction data. Details of these reactions, such as the target nuclei used, the incident energies are given in Table. 2. The theoretical predicted

single-nucleon removal cross sections using the NTG and the OLA, $\sigma_{-1N}^{\text{NTG}}$ and $\sigma_{-1N}^{\text{OLA}}$, respectively, are also listed together with the experimental single-nucleon removal cross sections, $\sigma_{-1N}^{\text{exp}}$, and the reduction factors, R_s^{NTG} and R_s^{OLA} , respectively. The single-particle spectroscopic factors (C^2S) used in these calculations are taken from references corresponding the experimental data and Refs. [41]. These reduction factors are depicted in Fig. 4 as functions of the neutron-proton asymmetry ΔS . In all these calculations, the single particle wave functions are calculated with Woods-Saxon potentials whose radius parameters, r_0 , are determined with the HF calculations [40] and the diffuseness parameters being fixed as $a = 0.65$ fm except for the $^{15,17,18}\text{C}$ projectiles, for which, the $r_0 = 1.15$ fm and $a = 0.50$ fm is used following Ref. [42]. And for proton removal of ^{16}C , $r_0 = 1.40$ fm and $a = 0.70$ fm is used following Ref. [43]. The proton and neutron density distributions of the ^9Be nucleus are taken to be a Gaussian form with a root-mean-square radius of 2.36 fm [9].

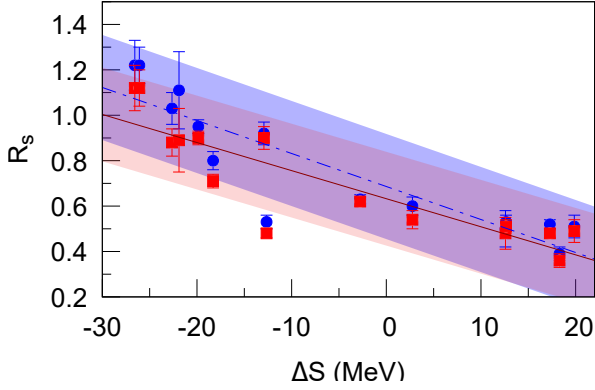


Fig. 4. The averaged reduction factors R_s listed in Table. 2 as a function of the neutron-proton asymmetry ΔS . The red squares and blue dots are results of the NTG method and the OLA, respectively. The widths of light red and blue bands represent their corresponding χ^2 .

As one can see from Table. 2, the NTG method predicted σ_{-1N} values are generally larger than those of OLA, leading to smaller R_s values than those of the latter. On average, the changes induced by NTG with respect to the OLA is about 7.8%. The averaged reduction factors, R_s^{NTG} and R_s^{OLA} , as shown in Fig. 4 still show linear dependence on the neutron-proton asymmetry ΔS with slightly different slopes:

$$\begin{aligned} R_s^{\text{OLA}} &= 0.686 - 0.0145\Delta S \\ R_s^{\text{NTG}} &= 0.633 - 0.0124\Delta S \end{aligned} \quad (25)$$

So the systematics of the R_s values with respect to ΔS observed in Refs. [8, 9] persist even when the multiple scattering effect is dealt with using the NTG method in the Glauber model calculations.

IV. SUMMARY

The reduction of the single-particle strengths, represented by the reduction factors of single-nucleon spectroscopic factors extracted from experimental data with respect to configuration interaction shell model predictions, is supposed to be related to the nucleon-nucleon correlations in atomic nuclei. Quite a lot of theoretical and experimental efforts have been devoted to this area. One of the open questions is why the the reduction factors obtained from intermediate- and high-energy single nucleon removal cross sections as those compiled in Refs. [8, 9] show strong linear dependence on the neutron-proton asymmetry, whereas those of other types of reactions, such as (p,pN) and single nucleon transfer reactions do not [2, 3, 6, 57–59]. Since the single-nucleon removal reactions are analyzed with the Glauber model. The validity of the Glauber model on such reactions is being questioned. With this respect, corrections to the Glauber model and examination of their effects on the single-nucleon removal cross sections becomes important.

In this work, we examine how the nucleon-target version of the Glauber model, which, compared with the widely used optical limit approximation, introduces multiple scattering of the constituent nucleons in the projectile and the target nuclei, could change the theoretical predicted single-nucleon removal cross sections. For this purpose, we firstly examined, and verified that the NTG method is of advantageous with respect to the OLA in their reproduction of the elastic scattering angular distributions and the total reaction cross sections of the experimental data of the $^{12}\text{C} + ^{12}\text{C}$ system, which is in agreement with the previous publications, e.g., Refs. [15, 17, 23].

We then compare the predictions of inclusive single-nucleon removal cross sections by using the NTG method and OLA with the $(^{19}\text{C}, ^{18}\text{C})$ reaction within the incident energy range from 50 to 400 MeV/nucleon. It is found that the NTG over-predicted the OLA cross sections within the whole energy range. The difference is found to be larger at lower incident energies. It will also be larger when the separation energy of the nucleon is larger, which correspond to a smaller root-mean-square radius of the single-particle wave function.

Finally, we study how much the reduction factors of the single particle strengths obtained from single-nucleon removal reactions induced by ^{9-20}C isotopes on carbon and Be targets using the NTG method and the OLA. On average, the reduction factors obtained with the NTG method are found to be less than those with the OLA by 7.8%. However, their linear dependence on the neutron-proton asymmetry persists. Thus, the question of why the reduction factors of the single particle strengths from single-nucleon removal reaction measurements depend differently on ΔS with respect to other types of reactions remains open even when the multiple scattering effect is included in the Glauber model analysis with the NTG method.

TABLE 2. Experimental ($\sigma_{-1N}^{\text{exp}}$) and theoretical inclusive single-nucleon removal cross sections calculated with the OLA ($\sigma_{-1N}^{\text{OLA}}$) and the NTG method ($\sigma_{-1N}^{\text{NTG}}$), and the corresponding reductions factors R_s .

Reaction	ΔS	Target	E_{inc}	$\sigma_{-1N}^{\text{exp}}$	$\sigma_{-1N}^{\text{OLA}}$	$\sigma_{-1N}^{\text{NTG}}$	R_s^{OLA}	R_s^{NTG}
($^{20}\text{C}, ^{19}\text{C}$)	-26.57	C	240	58(5) [44]	47.55	51.88	1.22(11)	1.12(10)
($^{19}\text{C}, ^{18}\text{C}$)	-26.09	Be	57	264(80) [45]	179.06	201.62	1.47(45)	1.31(40)
		Be	64	226(65) [46]	176.69	195.48	1.28(37)	1.16(33)
		C	243	163(12) [44]	134.75	146.63	1.21(9)	1.11(8)
		Average					1.22(8)	1.12(8)
($^{17}\text{C}, ^{16}\text{C}$)	-22.64	C	49	84(8) [42]	92.80	109.70	0.91(9)	0.77(7)
		Be	62	115(14) [45]	87.80	100.77	1.31(16)	1.14(14)
		Be	79	116(18) [47]	90.37	100.48	1.28(20)	1.15(18)
Average							1.03(7)	0.88(6)
($^{18}\text{C}, ^{17}\text{C}$)	-21.90	C	43	115(18) [42]	103.20	128.70	1.11(17)	0.89(14)
($^{15}\text{C}, ^{14}\text{C}$)	-19.86	C	54	137(16) [42]	180.56	196.44	0.76(9)	0.70(8)
		C	62	159(15) [42]	176.11	189.78	0.90(8)	0.84(8)
		C	83	146(23) [31]	166.44	176.08	0.88(14)	0.83(13)
		Be	103	146(23) [46]	142.52	149.89	0.98(3)	0.94(3)
		Average					0.95(3)	0.90(0)
($^{16}\text{C}, ^{15}\text{C}$)	-18.30	C	55	65(6) [42]	90.90	103.73	0.72(7)	0.63(6)
		C	62	77(9) [42]	89.78	101.10	0.86(10)	0.76(9)
		Be	75	81(7) [43]	81.99	90.94	0.99(9)	0.89(8)
		C	83	65(5) [45]	86.75	94.87	0.75(6)	0.69(5)
		Average					0.80(4)	0.71(3)
Average								
($^9\text{C}, ^8\text{B}$)	-12.93	Be	67	48.6(73) [48]	62.77	66.67	0.77(12)	0.73(11)
		Be	100	56(3) [49]	58.77	59.72	0.95(5)	0.94(5)
Average							0.92(5)	0.90(5)
($^{14}\text{C}, ^{13}\text{C}$)	-12.65	C	67	65(4) [42]	133.284	148.61	0.49(3)	0.44(3)
		C	83	67(14) [31]	130.74	142.66	0.51(13)	0.47(12)
		C	235	80(7) [50]	110.92	121.39	0.72(6)	0.66(6)
Average							0.53(3)	0.48(2)
($^{12}\text{C}, ^{11}\text{B}$)	-2.76	C	230	63.9(66) [51]	103.75	105.33	0.62(6)	0.61(6)
		C	250	65.6(26) [52]	102.93	105.36	0.64(3)	0.62(2)
Average							0.63(2)	0.62(2)
($^{12}\text{C}, ^{11}\text{C}$)	2.76	C	95	53(22) [53]	102.21	111.06	0.52(22)	0.48(20)
		C	240	60.51(11.08) [54]	94.12	104.37	0.64(12)	0.58(11)
		C	250	56.0(41) [52]	93.73	104.31	0.60(4)	0.54(4)
Average							0.60(4)	0.54(4)
($^{13}\text{C}, ^{12}\text{B}$)	12.59	C	234	39.5(60) [51]	79.69	81.55	0.43(5)	0.40(4)
($^{14}\text{C}, ^{13}\text{B}$)	12.65	C	235	41.3(27) [51]	78.65	81.43	0.53(3)	0.51(3)
($^{10}\text{C}, ^9\text{C}$)	17.28	Be	120	23.4(11) [55]	47.40	51.65	0.49(2)	0.45(2)
		C	120	27.4(13) [55]	49.72	54.36	0.55(3)	0.50(2)
Average							0.52(2)	0.48(2)
($^{16}\text{C}, ^{15}\text{B}$)	18.30	Be	75	18(2) [43]	44.97	47.21	0.40(4)	0.38(4)
		Be	239	16(2) [56]	45.09	47.52	0.35(4)	0.34(4)
		C	239	18(2) [51]	42.06	44.69	0.43(5)	0.40(4)
Average							0.39(3)	0.36(3)
($^{15}\text{C}, ^{14}\text{B}$)	19.86	C	237	28.4(28) [51]	55.36	57.58	0.51(5)	0.49(5)

ACKNOWLEDGMENTS

This work was financially supported by the National Key R&D Program of China (Grant No. 2023YFA1606702)

and the National Natural Science Foundation of China (Nos. U2067205 and 12205098).

- [1] N. K. Glendenning, in *Direct Nuclear Reactions*, (WORLD SCIENTIFIC, 2004)
- [2] B. P. Kay, J. P. Schiffer, S. J. Freeman, Quenching of cross sections in nucleon transfer reactions, *Phys. Rev. Lett.*, **111**: 042502 (2013). DOI:10.1103/PhysRevLett.111.042502
- [3] B. P. Kay, T. L. Tang, I. A. Tolstukhin, *et al.*, Quenching of single-particle strength in $a = 15$ nuclei, *Phys. Rev. Lett.*, **129**: 152501 (2022). DOI:10.1103/PhysRevLett.129.152501
- [4] V. R. Pharipe, I. Sick, P. K. A. d. Huberts, Independent particle motion correlations in fermion systems, *Rev. Mod. Phys.*, **69**,981–991 (1997). DOI:10.1103/RevModPhys.69.981
- [5] W. Dickhoff C. Barbieri, Self-consistent green's function method for nuclei nuclear matter, *Progress in Particle Nuclear Physics*, **52**,377–496 (2004). DOI:10.1016/j.ppnp.2004.02.038
- [6] L. Atar, S. Paschalis, C. Barbieri, *et al.*, Quasifree (p , $2p$) reactions on oxygen isotopes: Observation of isospin independence of the reduced single-particle strength, *Phys. Rev. Lett.*, **120**: 052501 (2018). DOI:10.1103/PhysRevLett.120.052501
- [7] F. Flavigny, N. Keeley, A. Gillibert, A. Obertelli, Single-particle strength from nucleon transfer in oxygen isotopes: Sensitivity to model parameters, *Phys. Rev. C*, **97**: 034601 (2018). DOI:10.1103/PhysRevC.97.034601
- [8] J. A. Tostevin A. Gade, Systematics of intermediate-energy single-nucleon removal cross sections, *Phys. Rev. C*, **90**: 057602 (2014). DOI:10.1103/PhysRevC.90.057602
- [9] J. A. Tostevin A. Gade, Updated systematics of intermediate-energy single-nucleon removal cross sections, *Phys. Rev. C*, **103**: 054610 (2021). DOI:10.1103/PhysRevC.103.054610
- [10] P. Hansen J. Tostevin, Direct reactions with exotic nuclei, *Annual Review of Nuclear Particle Science*, **53** :219–261 (2003). DOI:10.1146/annurev.nucl.53.041002.110406
- [11] T. Pohl, Y. L. Sun, A. Obertelli, *et al.*, Multiple mechanisms in proton-induced nucleon removal at ~ 100 MeV/Nucleon, *Phys. Rev. Lett.*, **130**: 172501 (2023). DOI:10.1103/PhysRevLett.130.172501
- [12] E. C. Simpson J. A. Tostevin, One- two-neutron removal from the neutron-rich carbon isotopes, *Phys. Rev. C*, **79**: 024616 (2009). DOI:10.1103/PhysRevC.79.024616
- [13] C. Bertulani, Core destruction in knockout reactions, *Physics Letters B*, **846**: 138250 (2023). DOI:10.1016/j.physletb.2023.138250
- [14] Y. Suzuki, K. Yabana, R. G. Lovas, K. Varga, in *Structure Reactions of Light Exotic Nuclei*, (Taylor & Francis, 2003).
- [15] B. Abu-Ibrahim Y. Suzuki, Scatterings of complex nuclei in the glauher model, *Phys. Rev. C*, **62**: 034608 (2000). DOI:10.1103/PhysRevC.62.034608
- [16] B. Abu-Ibrahim Y. Suzuki, Utility of nucleon-target profile function in cross section calculations, *Phys. Rev. C*, **61**: 051601 (2000). DOI:10.1103/PhysRevC.61.051601
- [17] W. Horiuchi1, Y. Suzuki, B. Abu-Ibrahim *et al.*, Systematic analysis of reaction cross sections of carbon isotopes, *Phys. Rev. C*, **76**: 039903 (2000). DOI:10.1103/PhysRevC.75.044607
- [18] R. J. Glauber, in *Lectures on Theoretical Physics*, (Interscience, New York, 1959)
- [19] L. Ray, Proton-nucleus total cross sections in the intermediate energy range, *Phys. Rev. C*, **20**:1857–1872, (1979). DOI:10.1103/PhysRevC.20.1857
- [20] C. Werneth, X. Xu, R. Norman, W. Ford, K. Maung, Validation of elastic cross section models for space radiation applications, *Nuclear Instruments Methods in Physics Research Section B: Beam Interactions with Materials Atoms*, **392**,74–93 (2017). DOI:10.1016/j.nimb.2016.12.009
- [21] R. L. Workman *et al.*, Review of particle physics, *PTEP*, **2022**: 083C01 (2022). DOI:10.1093/ptep/ptac097
- [22] J. A. Tostevin, Cross sections of removal reactions populating weakly-bound residual nuclei , (2022). DOI:10.48550/arXiv.2203.06058
- [23] T. Nagahisa W. Horiuchi, Examination of the ^{22}C radius determination with interaction cross sections, *Phys. Rev. C*, **97**: 054614 (2018). DOI:10.1103/PhysRevC.97.054614
- [24] C. Bertulani A. Gade, Momdis: a glauher model computer code for knockout reactions, *Computer Physics Communications*, **175** ,372–380 (2006). DOI:10.1016/j.cpc.2006.04.006
- [25] J.A. Tostevin, M.H. Lopes, and R.C. Johnson, Elastic scattering and deuteron-induced transfer reactions, *Nucl. Phys. A*, **465**: 83-122 (1984). DOI:10.1016/0375-9474(87)90300-9
- [26] M. Takechi, M. Fukuda, M. Mihara, *et al.*, Reaction cross sections at intermediate energies and Fermi-motion effect, *Phys. Rev. C*, **79**: 061601(R) (2009). DOI:10.1103/PhysRevC.79.061601
- [27] Y.H. Wang, D.Y. Pang, W.D. Chen, *et al.*, Nuclear radii from total reaction cross section measurements at intermediate energies with complex turning point corrections to the eikonal model, *Phys. Rev. C*, **109**: 014621 (2024). DOI:10.1103/PhysRevC.109.014621
- [28] J. Hostachy, M. Buenerd, J. Chauvin, *et al.*, Elastic inelastic scattering of ^{12}C ions at intermediate energies, *Nucl. Phys. A*, **490**,441–470 (1988). DOI:10.1016/0375-9474(88)90514-3
- [29] M. Buenerd, A. Lounis, J. Chauvin, D. Lebrun: Martin, G. Duhamel, J. Gondr, P. De Saintignon, Elastic inelastic scattering of carbon ions at intermediate energies, *Nucl. Phys. A*, **424**: 313–334 (1984). DOI:10.1016/0375-9474(84)90186-6
- [30] D.T. Khoa, α -nucleus optical potential in the double-folding model, *Phys. Rev. C*, **63**: 034007 (2018). DOI:10.1103/PhysRevC.63.034007
- [31] D. Q. Fang, T. Yamaguchi, T. Zheng, *et al.*, One-neutron halo structure in ^{15}C , *Phys. Rev. C*, **69**: 034613 (2004). DOI:10.1103/PhysRevC.69.034613
- [32] S. Kox, A. Gamp, C. Perrin, *et al.*, Trends of total reaction cross sections for heavy ion collisions in the intermediate energy range, *Phys. Rev. C*, **35**,1678–1691 (1987). DOI:10.1103/PhysRevC.35.1678
- [33] J. Jaros, A. Wagner, L. erson, *et al.*, Nucleus-nucleus total cross sections for light nuclei at 1.55 2.89 gev/c per nucleon, *Phys. Rev. C*, **18**,2273–2292 (1978). DOI:10.1103/PhysRevC.18.2273
- [34] T. Zheng, T. Yamaguchi, A. Ozawa, *et al.*, Study of halo structure of ^{16}C from reaction cross section measurement, *Nuclear Physics A*, **709**, 103–118 (2002). DOI:10.1016/S0375-

- 9474(02)01043-6
- [35] H. Zhang, W. Shen, Z. Ren, *et al.*, Measurement of reaction cross section for proton-rich nuclei ($a < 30$) at intermediate energies, *Nuclear Physics A*, **707**, 303–324 (2002). DOI:10.1016/S0375-9474(02)01007-2
- [36] C. Perrin, S. Kox, N. Longequeue, *et al.*, Direct measurement of the $^{12}\text{C} + ^{12}\text{C}$ reaction cross section between 10 and 83 mev/nucleon, *Phys. Rev. Lett.*, **49**, 1905–1909, (1982). DOI:10.1103/PhysRevLett.49.1905
- [37] M. Takechi, M. Fukuda, M. Mihara, *et al.*, Reaction cross-sections for stable nuclei nucleon density distribution of proton drip-line nucleus 8B, *The European Physical Journal A*, **25**, 217–219, (2005). DOI:10.1140/epjad/i2005-06-078-0
- [38] L. Ponnath, T. Aumann, C. Bertulani, *et al.*, Measurement of nuclear interaction cross sections towards neutron-skin thickness determination, *Physics Letters B*, **855**:138780 (2024). DOI:10.1016/j.physletb.2024.138780
- [39] K. Hencken, G. Bertsch, H. Esbensen, Breakup reactions of the halo nuclei ^{11}Be ^8B , *Phys. Rev. C*, **54**, 3043–3050 (1996). DOI:10.1103/PhysRevC.54.3043
- [40] W. L. Hai, D. Y. Pang, X. B. Wang, *et al.*, Determining the radii of single particle potentials with skyrme hartree fock calculations, *Phys. Rev. C*, **110**:044613 (2024). DOI:10.1103/PhysRevC.110.044613
- [41] Y.-P. Xu, D.-Y. Pang, C.-X. Yuan, X.-Y. Yun, Quenching of single-particle strengths of carbon isotopes 9-12,14-20c with knockout reactions for incident energies 43-2100 mev/nucleon *, *Chinese Physics C*, **46**: 064102 (2022). DOI:10.1088/1674-1137/ac5236
- [42] E. Sauvan, F. Carstoiu, N. A. Orr, *et al.*, One-neutron removal reactions on light neutron-rich nuclei, *Phys. Rev. C*, **69**: 044603 (2004). DOI:10.1103/PhysRevC.69.044603
- [43] F. Flavigny, A. Obertelli, A. Bonaccorso, *et al.*, Nonsudden limits of heavy-ion induced knockout reactions, *Phys. Rev. Lett.*, **108**: 252501 (2012). DOI:10.1103/PhysRevLett.108.252501
- [44] N. Kobayashi, T. Nakamura, J. A. Tostevin, *et al.*, One-two-neutron removal reactions from the most neutron-rich carbon isotopes, *Phys. Rev. C*, **86**: 054604 (2012). DOI:10.1103/PhysRevC.86.054604
- [45] V. Maddalena, T. Aumann, D. Bazin, *et al.*, Single-neutron knockout reactions: Application to the spectroscopy of $^{16,17,19}\text{C}$, *Phys. Rev. C*, **63**: 024613 (2001). DOI:10.1103/PhysRevC.63.024613
- [46] J. R. Terry, D. Bazin, B. A. Brown, *et al.*, Absolute spectroscopic factors from neutron knockout on the halo nucleus ^{15}C , *Phys. Rev. C*, **69**: 054306 (2004). DOI:10.1103/PhysRevC.69.054306
- [47] C. Wu, Y. Yamaguchi, A. Ozawa, I. Tanihata, D. Jiang, H. Hua, T. Zheng, Z. Li, Y. Ye, Neutron removal reactions of ^{17}C , *Journal of Physics G: Nuclear Particle Physics*, **31**: 39 (2004). DOI:10.1088/0954-3899/31/1/004
- [48] R. J. Charity, L. G. Sobotka, J. A. Tostevin, Single-nucleon knockout cross sections for reactions producing resonance states at or beyond the drip line, *Phys. Rev. C*, **102**: 044614 (2020). DOI:10.1103/PhysRevC.102.044614
- [49] D. Bazin, R. J. Charity, R. T. de Souza, *et al.*, Mechanisms in knockout reactions, *Phys. Rev. Lett.*, **102**: 232501 (2009). DOI:10.1103/PhysRevLett.102.232501
- [50] Y. Z. Sun, S. T. Wang, Z. Y. Sun, *et al.*, Single-neutron removal from $^{14,15,16}\text{C}$ near 240 mev/nucleon, *Phys. Rev. C*, **104**: 014310 (2021). DOI:10.1103/physrevc.104.014310
- [51] Y. Z. Sun, S. T. Wang, Z. Y. Sun, *et al.*, One-proton removal from neutron-rich carbon isotopes in $^{12-16}\text{C}$ beams near 240 mev/nucleon beam energy, *Phys. Rev. C*, **110**: 014603 (2024). DOI:10.1103/PhysRevC.110.014603
- [52] B. A. Brown: G. Hansen, B. M. Sherrill, J. A. Tostevin, Absolute spectroscopic factors from nuclear knockout reactions, *Phys. Rev. C*, **65**: 061601 (2002). DOI:10.1103/PhysRevC.65.061601
- [53] J. Dudouet, D. Juliani, M. Labalme, *et al.*, Double-differential fragmentation cross-section measurements of 95 mev/nucleon ^{12}C beams on thin targets for hadron therapy, *Phys. Rev. C*, **88**: 024606 (2013). DOI:10.1103/PhysRevC.88.024606
- [54] Y. SUN, Y. ZHAO, S. JIN, *et al.*, Data analysis framework for radioactive ion beam experiments at the external target facility of hirfl-csr, *Nuclear Physics Review*, **37**: 742 (2020). DOI:10.11804/NuclPhysRev.37.2019CNPC27
- [55] G. F. Grinyer, D. Bazin, A. Gade, *et al.*, Systematic study of p -shell nuclei via single-nucleon knockout reactions, *Phys. Rev. C*, **86**: 024315 2012. DOI:10.1103/PhysRevC.86.024315
- [56] Y. X. Zhao, Y. Z. Sun, S. T. Wang, *et al.*, One-proton knockout from ^{16}C at around 240 mev/nucleon, *Phys. Rev. C*, **100**: 044609 (2019). DOI:10.1103/PhysRevC.100.044609
- [57] F. Flavigny, A. Gillibert, L. Nalpas, *et al.*, Limited asymmetry dependence of correlations from single nucleon transfer, *Phys. Rev. Lett.*, **110**: 122503 (2013). DOI:10.1103/PhysRevLett.110.122503
- [58] M. Gómez-Ramos A. Moro, Binding-energy independence of reduced spectroscopic strengths derived from (p,2p) (p,pn) reactions with nitrogen oxygen isotopes, *Physics Letters B*, **785**, 511–516 (2018). DOI:10.1016/j.physletb.2018.08.058
- [59] Y.P. Xu, D.Y. Pang, X.Y. Yun, *et al.*, Proton–neutron asymmetry independence of reduced single-particle strengths derived from (p,d) reactions, *Physics Letters B*, **790**, 308–313 (2019). DOI:10.1016/j.physletb.2019.01.034